

Light Load Efficiency Improvement of Flying Capacitor-type Current-Fed DAB Converter for 1500V DC-grid

Takashi Ohno

Dept. of Science of Technology
Innovation
Nagaoka University of Technology
Nagaoka, Japan
s225058@stn.nagaokaut.ac.jp

Rintaro Kusui

Dept. of Science of Technology
Innovation
Nagaoka University of Technology
Nagaoka, Japan
kusui@stn.nagaokaut.ac.jp

Hiroki Watanabe

Dept. of Electrical, Electronics, and
Information Engineering
Nagaoka University of Technology
Nagaoka, Japan
hwatanabe@vos.nagaokaut.ac.jp

Jun-ichi Itoh

Dept. of Science of Technology
Innovation
Nagaoka University of Technology
Nagaoka, Japan
itoh@vos.nagaokaut.ac.jp

Abstract—This paper proposes a three-level current-fed dual active bridge (DAB) converter to achieve a wide high-efficiency range for DC voltage and load variation. The proposed control provides zero voltage switching (ZVS) by triangular current mode (TCM) under a wide DC voltage range. Additionally, the transformer root mean square (RMS) current is drastically reduced compared with the conventional control because the DC-voltage ratio is regulated by voltage control to match with the transformer turn ratio. Moreover, the proposed control improves the light load efficiency using the full-bridge (FB) and the half-bridge (HB) modes. The loss analysis results show that the proposed control reduces switching by 46%. The conduction losses were reduced by 53%. The proposed three-level current-fed DAB converter achieves an efficiency of 93.5% or higher over a wide voltage range from 160V to 320V. Finally, the experimental results indicated that the total loss is reduced by 63% at 0.2p.u.

Keywords—Current-fed dual active bridge converter, Multi-level, Wide range, Zero voltage switching, Triangular current mode, Medium voltage

I. INTRODUCTION

Recently, 1500-V DC grid systems connecting light rail transit (LRT), electric vehicles (EV), renewable energy sources, and so on are attracting attention from around the world for energy decarbonization policies [1][2]. In these systems, an isolated DC-DC converter has been widely developed to interface the converter between the 1500-V DC grid and energy sources or batteries [3][4]. A dual active bridge (DAB) converter is one of the strong candidates because there are attractive advantages, e.g., 1) galvanic isolation capability, 2) zero voltage switching (ZVS) operation for low switching losses, and 3) simple configuration. However, the DAB converter has a narrow high-efficiency range due to the soft switching failure and increasing circulating current under the DC voltage variation. Additionally, the large ripple current may increase the smoothing capacitor.

In[5]-[9], several modulation methods have been proposed to achieve ZVS, and current RMS reduction even when the voltage ratio does not agree with the turn-ratio of the transformer. The various modulation methods which are the expanding ZVS range[5]-[7] or achieving minimum

transformer current RMS[8][9], have been proposed. Specifically, extended-phase shift (EPS) control [5], dual-phase shift (DPS) control [6], and triple-phase shift (TPS) control [7] have been proposed as modulation method that achieves ZVS over a wide range and minimum current RMS. However, these methods require complicated calculation to find the optimal combination of the switching frequency, the phase shift angle of individual legs, and the phase shift angle of each bridge. In ref [10][11], the DAB converter with the multilevel topology of the T-type and the neutral point clump (NPC) converters have been proposed to reduce the transformer current. These circuits switch the voltage levels applied to the transformer to reduce the transformer current RMS. However, the T-type based three-level converter is not enough to achieve high withstand voltage. The NPC based three-level converter has many additional components. Additionally, these converters increase the volume of the soothing capacitor because of the large ripple current.

By contrast, a current-fed DAB converter combined with an interleaved boost chopper with an H-bridge of the DAB has been proposed to reduce transformer current [12]. The current-fed DAB converter controls the voltage ratio to agree with the turn ratio of the transformer by the boost capacitor voltage control. For this reason, the current-fed DAB converter achieves low RMS of the transformer current. The converter is controlled by the triangular current mode (TCM), which flows a small negative inductor current. Thereby, the current-fed DAB converter achieves ZVS for the lower-side switch of the boost chopper. However, TCM is controlled at a variable frequency to keep the negative current constant. Specifically, the switching frequency increases for light load because the inductor current ripple needs to be reduced. Thus, the light load efficiency is decreased due to the turn-off loss is increased at light load.

This paper proposes the current-fed DAB converter with the three-level flying capacitor (FC) converter to keep the high efficiency in load fluctuations and wide-range voltage conditions. The originality of this paper is that the flying capacitor type current-fed (FCCF) DAB converter reduces the switching loss by the switching operation of full-bridge and half-bridge mode. This paper demonstrates the detailed of loss

analysis, and experimental result with a 12.8-kW prototype to provide the effectiveness of the proposed control.

II. CIRCUIT CONFIGURATION

Fig. 1 shows the configuration of a DAB converter with a three-level flying capacitor (FC DAB). This converter consists a two-level inverter at the primary side and three-level flying capacitor inverter at the secondary side. The FC DAB converter is controlled by single phase shift modulation.

Fig. 2 shows the configuration of a current-fed DAB converter with a three-level flying-capacitor and an H-bridge integrated with the interleaved DC-DC converter. This converter controls the boost capacitor voltage so that the voltage ratio of the primary and the secondary sides to much the turn ratio of the transformer. This converter applies the triangular current mode (TCM) for boost inductor current of i_{LCA} and i_{LCB} in order to achieve ZVS in all switching of the primary side. Additionally, the phase shift angle of interleaved converter sets a 180-degree to significantly reduce the current ripple of the DC power sources.

Fig. 3 shows the operation waveform of the FCCF DAB converter. The conventional DAB converter sets the switching duty at 0.5. In contrast, the FCCF DAB converter changes the switching duty depending on the boost ratio. In addition, the FCCF DAB converter operates a variable switching frequency control to keep a constant negative current at TCM. However, the performance of the power device limits the switching frequency. In this paper, the frequency range is set from 10kHz to 30kHz. The relationship between switching frequency and input power is expressed as

$$f_s = \frac{V_{in}^2 D}{L_C (P_{in}^* - 2V_{in} I_{bot}^*)} \quad (10\text{kHz} \leq f_s \leq 30\text{kHz}) \quad (1),$$

where V_{in} is the input voltage, L_C is the boost inductor, P_{in}^* is the command of the input power, I_{bot}^* is the command of the boost inductor current bottom value, and D is defined as

$$D = 1 - \frac{V_{in}}{V_C} \quad (2),$$

where V_C is the boost capacitor voltage.

III. OPERATION MODE AND ANALYSIS

A. Full Bridge (FB) Mode

In Fig. 3, the switching pattern in the full bridge (FB) mode for the FCCF DAB converter is shown. The triangle carrier for Q_2 is the base carrier. The triangle carrier for Q_4 shifted by 180 degrees with the base carrier. The switching timing of Q_5 have a δ phase shift with the base carrier. The switching timing of Q_9 have a δ phase shift with the Q_4 carrier. According to Fig. 3, the switching devices of Q_9 and Q_{10} are synchronized switching in the upper arm. Similarly, the switching devices of Q_{11} and Q_{12} are synchronized switching in the lower arm. As a result, a three-level waveform with an amplitude equal to the peak value of the grid voltage (1500V) is applied to the transformer during FB mode. Thus, the voltage of the primary boost capacitor is set to 800V due to the winding turn ratio of 8:15. The power transmission in the FB mode is expressed as

$$P_{Tr} = \frac{1}{2\pi} \int_0^{2\pi} v_{Pri}(\theta) i_{Tr}(\theta) d\theta \quad (3),$$

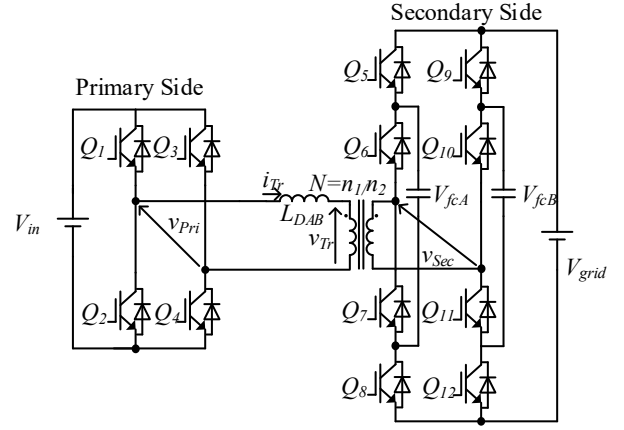


Figure 1. Conventional DAB converter with three-level flying capacitor (FC DAB)

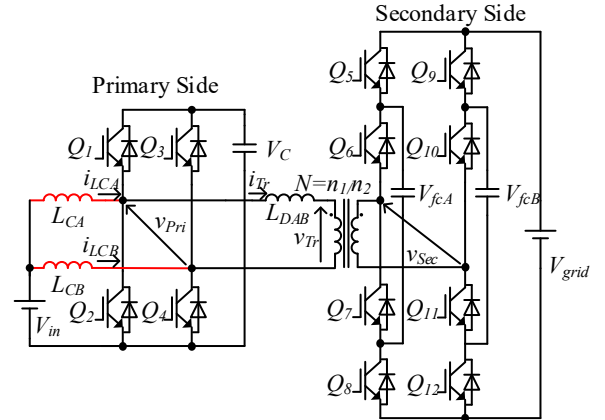


Figure 2. Proposed current-fed DAB converter with three-level flying capacitor (FCCF-DAB); V_{in} from 160V to 320V, V_{grid} 1500V, rated power 12.8kW.

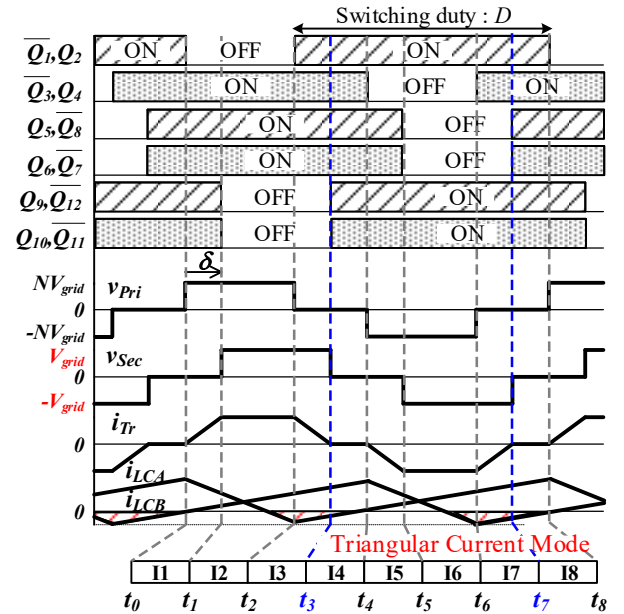


Figure 3. Key waveform of the FCCF DAB converter in the full bridge mode.

where P_{Tr} is the transmission power, v_{Pri} is the output voltage of the primary H-bridge, and i_{Tr} is the transformer current of the primary side. The phase shift angle is expressed from (3) as

$$\delta = \frac{2\pi}{V_C} \left\{ V_C - V_{in} - \sqrt{(V_C - V_{in})^2 - P^* f_S L_{DAB}} \right\} \quad (4).$$

Note that (4) is valid when $D < 0.5$. Furthermore, when the phase shift angle is larger than $(1-2D)\pi$, it is expressed as

$$\delta = \frac{\pi}{2V_C} \left\{ V_C - \sqrt{(-8D^2 + 8D - 1)V_C^2 - 8P^* f_S L_{DAB}} \right\} \quad (5).$$

Table 1 shows the switching condition in the FB mode. According to the table 1, the primary devices of Q_1 to Q_4 are achieved ZVS by the TCM. However, the secondary high-side devices of Q_5, Q_6, Q_9 , and Q_{10} does not achieved ZVS because the transformer current is zero at the switching timing. Note that the switching condition of the table 1 is valid for the power flow from the primary to the secondary sides. Thus, the lower side devices of Q_7, Q_8, Q_{11} , and Q_{12} does not achieved ZVS when the power flow from the secondary to the primary sides.

B. Half Bridge (HB) Mode

Fig. 4 shows the key waveform of the FCCF DAB converter in the HB mode. The HB mode outputs the flying capacitor voltage of 750V. Thus, the voltage of the primary-side boost capacitor is set to 400V in order to the voltage ratio to agree with the turn ratio of the transformer. In the HB mode, the switching patterns for discharging and charging are alternated to keep constant the flying capacitor voltage.

Table 2 shows the switching condition in the HB mode. The primary side devices of Q_1 to Q_4 are achieved ZVS by the TCM as in the FB mode. However, the HB mode does not achieved ZVS for the switching devices of Q_5, Q_6, Q_9 , and Q_{10} . The turn-on losses are only occurred by the energy charged into the output capacitance because the device current is zero.

C. Control block diagram of the FCCF DAB converter

Fig.5 shows the control block diagram of the FCCF DAB converter. The primary side of the FCCF DAB converter consists of the boost inductor current controller on the inner loop and the boost capacitor voltage controller on the outer loop. The boost capacitor command is switched by the operating mode to the FB mode of 800V and the HB mode of 400V. The voltage PI controller sends a command of the boost inductor current. The boost inductor current for both i_{LCA} and i_{LCB} are controlled with each current controller. The voltage command is calculated by the feedforward $(V_C - V_{in})$ from the output of the current PI controller. Furthermore, the switching duty D is calculated by normalizing the voltage command with boost capacitor voltage V_C . The secondary side of the FCCF DAB converter is used for the switching duty calculated on the primary side. The carrier frequency is calculated by the power command value into (1). The calculated switching frequency and power command are used in (4) to calculate the phase shift angle.

D. Loss Analysis with the FC DAB and the FCCF DAB converters

Table 3 shows the loss analysis and the experimental parameters in order to compare to the flying capacitor-type (FC) three-level DAB converter of conventional circuit and the FCCF DAB converter. The input voltage is 160V to 320V and the dc grid voltage is 1500V. The rated power is 12.8-kW with a maximum input current limited to 40A because it is designed for the battery applications. The switching frequencies are designed to agree with the switching

Table 1. the switching condition in the FB mode

timing	i_{LCA}	i_{LCB}	i_{Tr}	Turn on
t_0	positive	-	zero	Q_1 : ZVS
t_1	-	-	positive	Q_{11}, Q_{12} : ZVS
t_2	negative	-	positive	Q_2 : ZVS
t_3	-	-	zero	Q_9, Q_{10} : Non-ZVS
t_4	-	positive	zero	Q_3 : ZVS
t_5	-	-	negative	Q_7, Q_8 : ZVS
t_6	-	negative	negative	Q_4 : ZVS
t_7	-	-	zero	Q_5, Q_6 : Non-ZVS

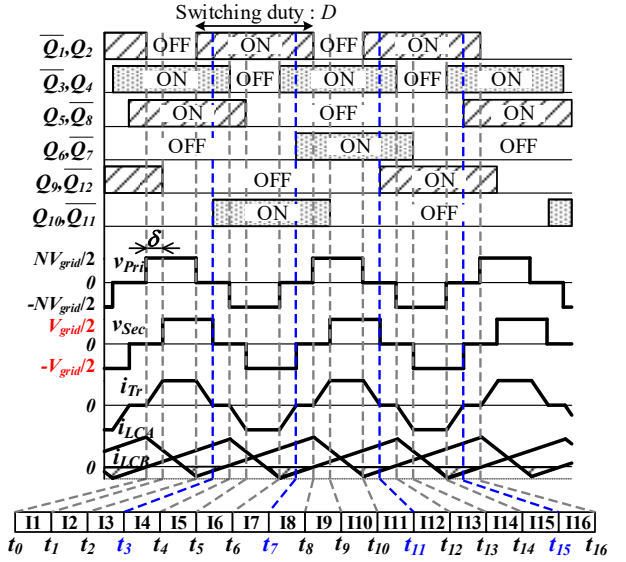


Figure 4. Key waveform of the FCCF DAB converter in the half bridge mode.

Table 2. the switching condition in the HB mode

timing	i_{LCA}	i_{LCB}	i_{Tr}	Turn on
t_0	positive	-	zero	Q_1 : ZVS
t_1	-	-	positive	Q_{12} : ZVS
t_2	negative	-	positive	Q_2 : ZVS
t_3	-	-	zero	Q_{10} : Non ZVS
t_4	-	positive	zero	Q_3 : ZVS
t_5	-	-	negative	Q_8 : ZVS
t_6	-	negative	negative	Q_4 : ZVS
t_7	-	-	zero	Q_6 : Non ZVS
t_8	positive	-	zero	Q_1 : ZVS
t_9	-	-	positive	Q_{11} : ZVS
t_{10}	negative	-	positive	Q_2 : ZVS
t_{11}	-	-	zero	Q_9 : Non ZVS
t_{12}	-	positive	zero	Q_3 : ZVS
t_{13}	-	-	negative	Q_7 : ZVS
t_{14}	-	negative	negative	Q_4 : ZVS
t_{15}	-	-	zero	Q_5 : Non ZVS

frequency at rated power between the FCCF DAB and the FC DAB. The sum of the inductance which is connected in series with the transformer is 68.5uH. The transformer winding turn ratios are designed to agree with the nominal voltage between the FCCF DAB and the FC DAB. In addition, the FCCF and

the FC DAB transformers are designed to match the maximum magnetic flux amplitude at rated condition. The switching device of the FCCF DAB converter and the FC DAB converter is the hybrid SiC modules (IGBT + SiC SBD: CMH150DY-24NFH, MITSUBISHI ELECTRIC).

Fig. 6 shows the converter loss comparison of the FCCF DAB and FC DAB converters at the input voltage of 320V. The turn-on switching losses become zero at achieving an ideal ZVS condition because the energy of the output capacitance of the IGBT is regenerated to the power supply or sent to the load. However, the other switching losses occur such as the loss caused by a tail current. The output power of 1.0p.u. is out of the operating range in the HB mode under the rated power condition. For this reason, only the FB mode is compared at the rated power operation. From Fig. 6, the FCCF DAB converter has lower secondary side switching losses than the FC DAB converter because the FCCF DAB converter reduces the switching device current at turn-off. Similarly, the FCCF DAB converter has lower condition loss at the rated operating point by reduction of the RMS value of the transformer current.

IV. EXPERIMENTAL RESULT

A. Comparison of the FB and HB modes waveform

Fig. 7 shows the operation waveforms of the FCCF DAB converter with the FB and the HB modes at discharging operation. Fig. 7 shows the primary H-bridge voltage v_{Pri} , the secondary H-bridge voltage v_{Sec} , the primary transformer current i_{Tr} , and the boost inductor current i_{LCA} and i_{LCB} . Fig 7(a), (c) and (e) show the FB mode waveforms for the input voltage $V_{in} = 160V$, $V_{in} = 240V$ and $V_{in} = 320V$, respectively. Fig. 7(b), (d) and (f) show the HB mode waveforms. The input current I_{in} is the same at 0.5 p.u. (20A). In Fig. 7(a), (c) and (e), the amplitude of the primary-side H-bridge voltage is 800V. The secondary-side transformer voltage is the grid voltage (1500V), as in Fig. 3. In Fig. 7(b), (d) and (f), the amplitude of the primary-side H-bridge voltage is 400V. The secondary-side transformer voltage is half of the dc grid voltage (750V). The input current I_{in} is the same at 0.5p.u. (20A).

The switching duty of the FCCF DAB converter is decided by the relationship between the input voltage and the boost voltage. Specifically, the voltage ratio agrees with the turn ratio by the boost operation of the primary side. Therefore, the switching duty of the FCCF DAB converter is varied from 0.2 to 0.8. In addition, the boost inductor current is controlled by a variable switching frequency for the TCM operation. In Fig. 7(a) and (d), the switching frequency is reduced by the HB mode from 18.2kHz to 13.7kHz. In Fig. 7(b) and (e), the switching frequency is reduced from 23.9kHz to 13.7kHz. In Fig. 7(c) and (f), the switching frequency is reduced from 27.4kHz to 10kHz at 0.5p.u.

According to fig. 3 and fig. 4, all devices of the FCCF DAB converter are achieved ZVS on the primary side. The experimental results of fig. 7(a), (b) and (c) show no surge voltage at the switching timing of the primary H-bridge. However, the secondary upper arm devices of the FCCF DAB converter are not achieved ZVS. Therefore, the secondary side voltage of fig. 7(a), (b) and (c) occurs a surge voltage. Similarly, the primary devices of the HB mode are achieved ZVS. In contrast, the secondary upper arm devices are not achieved ZVS. Thus, there is occurred the surge voltage, as shown in fig. 7(d), (e) and (f).

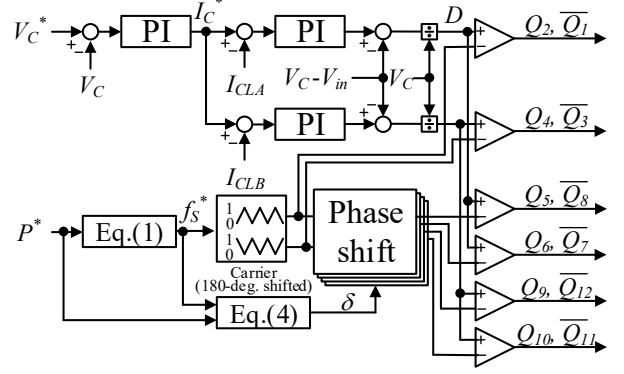


Figure 5. Control block diagram of the FCCF DAB converter.

Table 3. Loss analysis and experimental parameters

Element	Symbol	Value	
		FCCF DAB	FC DAB
Rated power	P_{rated}	12.8kW @ $V_{in}=320V$	
Rated current	I_{rated}	40A	
Switching frequency	f_s	10-30kHz	15kHz
Input voltage	V_{in}	160-320V	
DC-grid voltage	V_{grid}	1500V	
Boost capacitor voltage	V_C	(HB) 400V	–
		(FB) 800V	–
Boost inductor	L_C	270μH	–
External inductor	L_{EX}	45μH	64.5μH
Leakage Inductor	L_l	23.5μH	4.0μH
Magnetizing Inductance	L_{Mg}	48mH	2.6mH
Turn ratio	N	0.532	0.26
Dead-time	T_d	1μs	
Hybrid-SiC Modules	–	CMH150DY-24NFH	

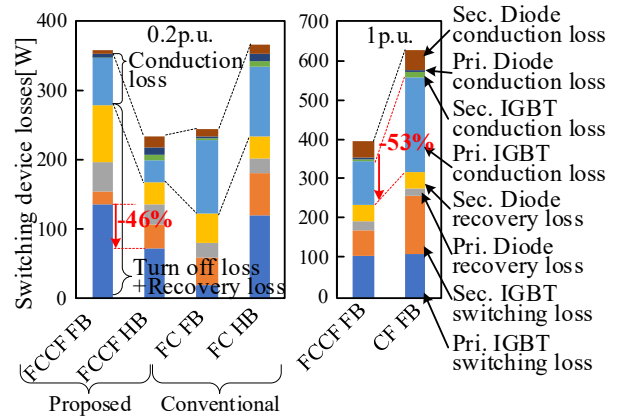


Figure 6. The converter loss comparison of the FCCF DAB and FC DAB converters at input voltage of 320V

B. Efficiency characteristics

Fig. 8 shows the efficiency characteristics of the 12.8-kW prototype. Fig. 8 indicates the input voltage characteristics at rated input current of 40A. The proposed control achieves a high-efficiency operation of up to 93.5% under the wide range voltage condition from 160V to 320V and the rated current

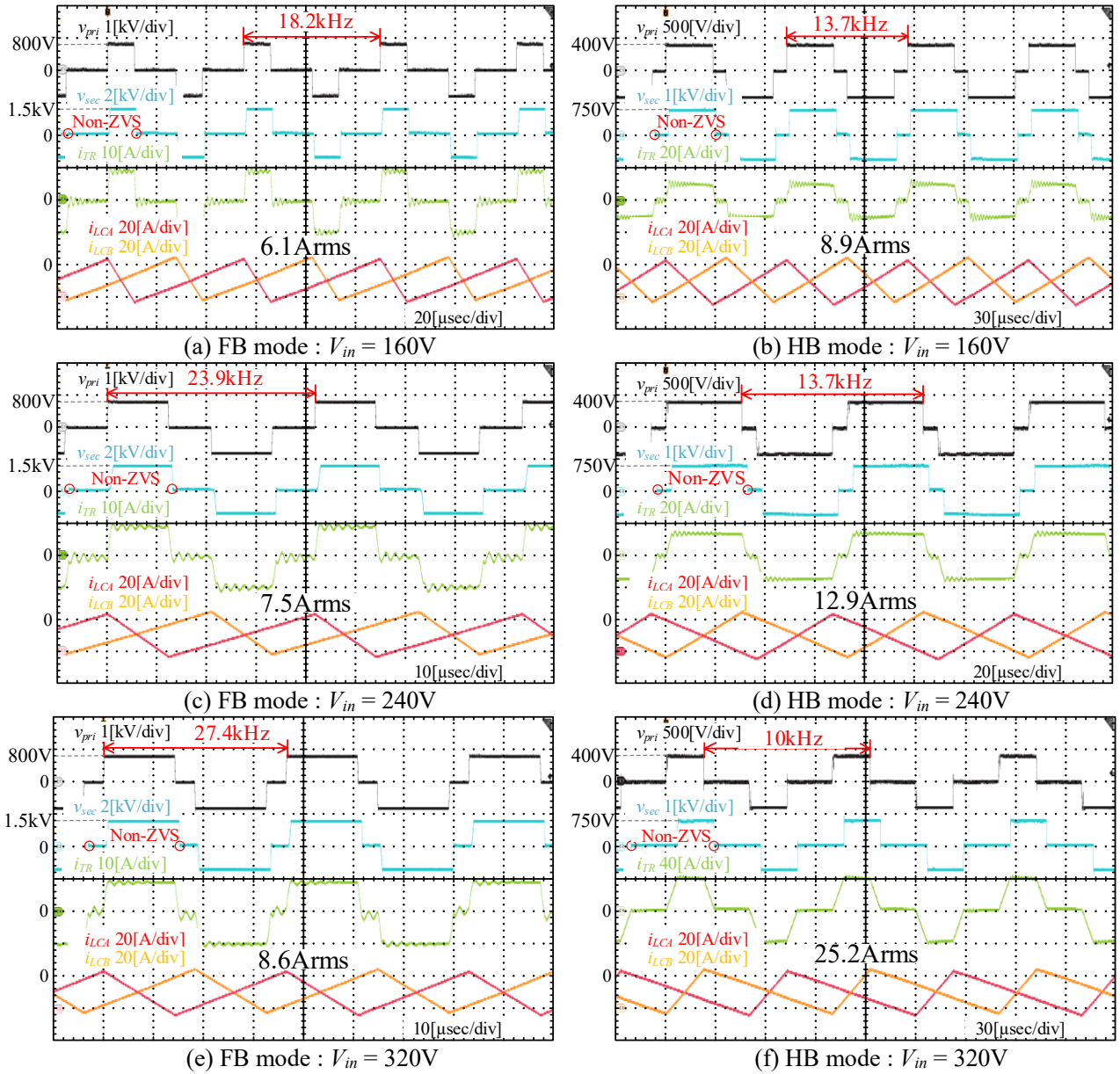


Figure 7. operation waveform of the FCCF DAB converter

condition. In contrast, the conventional circuit of the FC DAB converter has low efficiency compared to the FCCF DAB converter. The main factor is that the FC DAB converter operates under the condition where the transformer turn ratio and voltage ratio did not match. As a result, particularly under the low voltage conditions, there is an increase in the RMS value of the transformer current leading to reduced efficiency.

Fig. 9 shows the efficiency characteristics of the output power characteristics at an input voltage of 160V, 240V and 320V conditions. Fig. 9(a) shows the efficiency characteristics of the proposed circuit and the conventional circuit in the FB and the HB modes at input voltage of 160V. The HB mode of the FCCF DAB converter shows the highest efficiency across nearly all operation points. Similarly, the HB mode of the FC DAB converter shows relatively high-efficiency characteristics. However, it experiences a sharp dropped in efficiency around 0.5 p.u. The reason for this is that the phase shift angles on both the primary and the secondary sides have increased. As a result, the reactive power is increased due to the transformer current is increased. Furthermore, the converter efficiency of FB mode is significantly reduced due

to a deviation from a voltage ratio of 1.0. The converter occurs of increasing transformer current RMS and hard switching.

Fig. 9(b) shows the efficiency characteristics at an input voltage of 240V. The efficiency characteristics in the FB mode of the FC DAB converter and the FCCF DAB converter are nearly the same. However, in the HB mode, the FC DAB converter shows higher efficiency under very light load conditions, but the efficiency of the FCCF DAB converter becomes higher at a rated current exceeding 0.6p.u. The reason for the high efficiency of the FC DAB converter is the favorable input-to-output voltage ratio. However, the FCCF DAB converter keeps high efficiency even under high load conditions because the voltage ratio matches completely.

Fig. 9(c) shows the efficiency characteristics at an input voltage of 320V. The HB mode of the FCCF DAB converter improved light load efficiency because the HB mode operates at a lower switching frequency compared to the FB mode to reduce turn-off losses. As a result, the loss is reduced by 63% from the FB mode to the HB mode at 0.2p.u. condition. However, the FC DAB converter achieved higher efficiency compared to the FCCF DAB converter at almost all of the

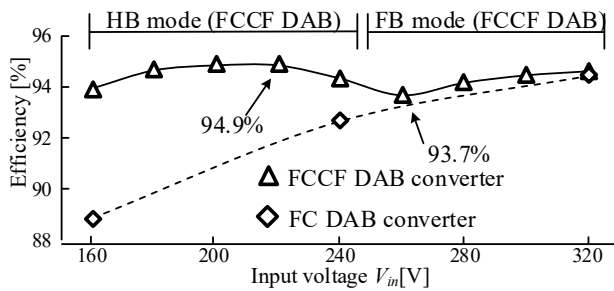


Figure 8. Efficiency characteristics of the voltage fluctuations at rated input current of 40A

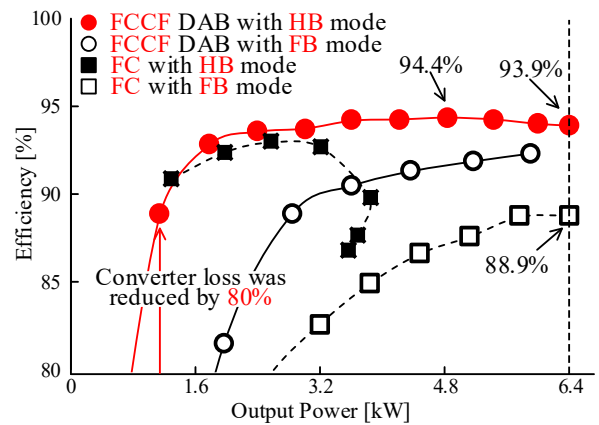
operating points. One of the reason is that the operating frequency of the FC DAB converter differs from the FCCF DAB converter by up to twice. Thus, it is supposed that the efficiency of the FCCF DAB converter decreases because of the increased switching losses during turn-off.

V. CONCLUSIONS

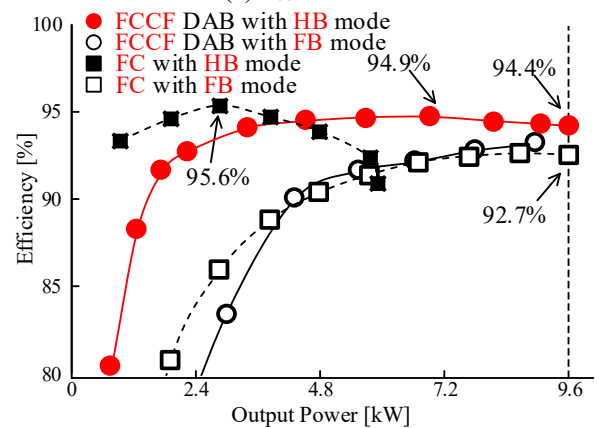
This paper proposed a three-level flying capacitor current-fed DAB converter for medium voltage applications(1500Vdc). The loss analysis results show that the HB mode of the FCCF DAB converter reduces the loss by 3.8% compared to the FC DAB with the HB mode of the conventional method at 0.2p.u. and the FB mode reduces the loss by 36.4% at 1.0p.u. Additionally, the experiment results show that the losses are reduced by 63% under the input voltage condition of 320V and the output power condition of 0.2p.u. Also, the FCCF DAB converter is achieved an efficiency of up to 93.5% under voltage variations from 160V to 320V and rated input current conditions. In future work, clarification of the switching point between the FB and the HB modes will be conducted.

REFERENCES

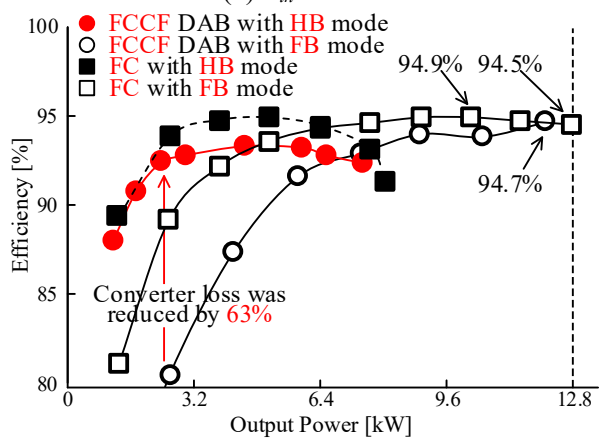
- [1] X. Huang, J. Zhao, F. Li, and F. Lin "Loss Characteristics of Input-Series Output-Parallel SiC DC-DC Converter Used in Auxiliary Power Systems," IEEJ Journal of Industry Applications, Vol. 8, No. 4, pp.677-684 (2019)
- [2] H. Heydari-doostabad and T. O'Fonnell "A Wide-Range High-Voltage-Gain Bidirectional DC-DC Converter for V2G and G2V Hybrid EV charger," IEEE Transaction on Industry Electronics, Vol. 69, No. 5, pp. 4718-4729 (2022)
- [3] T. Ishibashi, T. Jimichi, O. Mori "Circuit Topology and Control Scheme of a High-Power High-Voltage DC/DC Converter for Large Scale Offshore Wind Project with DC Collector Grids," IEEJ Trans. on Industry Applications, Vol. 138, No.1, pp.58-66 (2018)
- [4] B. Stevanovic, D. Serrano, M. Vasic, P. Alou, J. A. Oliver, and J. A. Cobos, "Highly Efficient, Full ZVS, Hybrid, Multilevel DC/DC Topology for Two-Stage Grid-Connected 1500-V PV System With Employed 900-V SiC Devices," IEEE Journal of Emerging and Selected Topics in Power Electronics, Vol. 7, No. 2, pp. 811-832 (2019)
- [5] G. Xu, L. Li, X. Chen, Y. Liu, Y. Sun, and M. Su, "Optimized EPS Control to Achieve Full Load Range ZVS With Seamless Transition for Dual Active Bridge Converter," IEEE Trans. on Industrial Electronics, Vol. 68, No. 9, pp. 8379-8390 (2021)
- [6] H. Bai, and C. Mi, "Eliminate Reactive Power and Increase System Efficiency of Isolated Bidirectional Dual-Active-Bridge Converters Using Novel Dual-Phase-Shift Control," IEEE Trans. on Industrial Electronics, Vol. 23, No. 6, pp. 2905-2914 (2008)
- [7] J. Huang, Y. Wang, Z. Li, and W. Lei, "Unified Triple-Phase-Shift Control to Minimize Current Stress and Achieve Full Soft-Switching of Isolated Bidirectional DC-DC Converter," IEEE Trans. on Industrial Electronics, Vol. 63, No. 7, pp. 4169-4179 (2016)
- [8] P. Liu, and S. Duan, "A Hybrid Modulation Strategy Providing Lower Inductor Current for the DAB Converter With the Aid of DC Blocking



(a) $V_{in} = 160V$



(b) $V_{in} = 240V$



(c) $V_{in} = 320V$

Figure 9. Efficiency characteristics of the output power at input voltage of 160V, 240V and 320V conditions.

Capacitor," IEEE Trans. on Power Electronics, Vol. 35, No. 4, pp. 4309-4319 (2020)

- [9] F. Krismer, and J. W. Kolar, "Closed Form Solution for Minimum Conduction Loss Modulation of DAB Converters," IEEE Trans. on Power Electronics, Vol. 27, No. 1, pp. 174-188 (2012)
- [10] H. Higa, S. Takuma, K. Kusaka, and J. Itoh, "Development of T-type Dual Active Bridge DC-DC Converter with Switching Operation Mode Over Wide-Voltage-Operation Range," IEEJ Trans. on Industry Applications, Vol. 139, No. 4, pp. 388-400 (2018)
- [11] A. F. Martinez, S. B. Monge, J. N. Apruzzese, and J. Bordonau, "Operating Principle and Performance Optimization of a Three-level NPC Dual-Active-Bridge DC-DC Converter," IEEE Trans. on Industrial Electronics, Vol. 63, No. 2, pp.678-690 (2016)
- [12] H. Watanabe, A. Tamagawa, and J. Itoh, "Efficiency Improvement of Current-Fed DAB Converter by Triangular Current Mode for Wide Voltage Applications," The 2022 International Power Electronics Conference (IPEC-Himeji 2022 ECC-Asia (2022)